Novel Interaction of the Voltage-Dependent Sodium Channel (VDSC) with Calmodulin: Does VDSC Acquire Calmodulin-Mediated Ca^{2+}-Sensitivity?†

Masayuki Mori,[‡,§] Takashi Konno,[∥] Takeaki Ozawa,[⊥] Masayuki Murata,[§] Keiji Imoto,[#] and Kuniaki Nagayama*[,‡,§]

Department of Physiological Sciences, The Graduate University for Advanced Studies, Department of Molecular Physiology, Center for Brain Experiment, and Department of Informational Physiology, National Institute for Physiological Sciences, Okazaki 444-8585, Japan, and Department of Chemistry, University of Tokyo, Tokyo 113-0033, Japan

Received June 2, 1999; Revised Manuscript Received September 21, 1999

ABSTRACT: The voltage-dependent sodium channel (VDSC) interacts with intracellular molecules to modulate channel properties and localizations in neuronal cells. To study protein interactions, we applied yeast two-hybrid screening to the cytoplasmic C-terminal domain of the main pore-forming α-subunit. We found a novel interaction between the C-terminal domain and calmodulin (CaM). By two-hybrid interaction assays, we specified the interaction site of VDSC in a C-terminal region, which is composed of 38 amino acid residues and contains both IQ-like and Baa motifs. Using a fusion protein of the C-terminal domain, we showed that interaction with CaM occurred in the presence and absence of Ca^{2+}. Two synthetic peptides, each covering the IQ-like (NaIQ) or the Baa motifs (NaBaa), were used to examine the binding property by a gel mobility shift assay. Although the NaIQ and NaBaa sequences are overlapped, NaBaa binds only to Ca^{2+}-bound Ca^{2+}CaM, whereas NaIQ binds to both Ca^{2+}CaM and Ca^{2+}-free apoCaM. Fluorescence spectroscopy of dansylated CaM showed Ca^{2+}-dependent spectral changes not only for NaBaa·CaM but also for NaIQ·CaM. The results, taken together with other results, indicate that whereas the NaBaa·CaM complex is formed in a Ca^{2+}-dependent manner, the NaIQ·CaM complex has two conformational states, distinct with respect to the peptide binding site and the CaM conformation, depending on the Ca^{2+} concentration. These observations suggest the possibility that VDSC is functionally modulated through the direct CaM interaction and the Ca^{2+}-dependent conformational transition of the complex.

The voltage-dependent sodium channel (VDSC)[1] is essential to generating action potentials in many excitable cells. The α-subunit of VDSC is the main component of the channel responsible for voltage-sensitive gating and selective ion permeation (*1*). This α-subunit could conceivably be modulated through interaction with associated proteins to regulate action potential generation. In fact, the electrophysiological response of VDSC type IIA, a splicing variant of VDSC type II (*2*), is modulated by direct binding of G protein subunits, $G\beta\gamma$, to the C-terminal domain of the channel protein (*3*). VDSC also interacts with the actin-associated proteins ankyrin and spectrin (*4*), which regulate channel localization, and AKAP15, which regulates phospholylation (*5*). Most of the above findings for the proteins interacting with VDSC are based, however, on indirect or functional observations.

To establish a solid biochemical basis for analyzing intracellular events regulating VDSC, we looked for proteins that directly interact with VDSC intracellularly, using yeast two-hybrid screening system (*6*), focusing on the C-terminal domain of VDSC type II. This domain is located intracellularly and exhibits a greater sequence diversity among the various α-subunits than in other regions of the protein.

Through yeast two-hybrid screening, we identified a novel interaction of VDSC with calmodulin (CaM). CaM, a ubiquitous small (16.7 kDa) calcium-binding protein, acts as an intracellular Ca^{2+} sensor, which translates Ca^{2+} signals into cellular responses by interacting with target molecules (*7*). Previous studies on the *Paramecium* calcium-dependent sodium channel showed that CaM binding to the channel itself or a channel-associated protein modulates activity of this type of sodium channel (*8*, *9*). In addition, recent observation has shown that the CaM interaction also modulates functions of other channels, such as the rod cGMP-gated cation channel (*10*, *11*), the *N*-methyl-D-aspartate (NMDA) receptor channel (*12*), the calcium-activated potassium channel (*13*), and the voltage-dependent calcium channels (VDCC) (*14*−*17*). Whereas their common feature is their coupling to cytoplasmic Ca^{2+} regulation, VDSC is not known to directly couple to the Ca^{2+} signaling. In this work, we studied the novel interaction of CaM and

† This work was supported in part by grants from the Ministry of Education, Science, Sports and Culture of Japan.

* Corresponding author. Telephone: +81-564-55-7811. Fax: +81-564-52-7913. E-mail: nagayama@nips.ac.jp.

‡ Department of Physiological Sciences, The Graduate University for Advanced Studies.

§ Department of Molecular Physiology, National Institute for Physiological Sciences.

∥ Center for Brain Experiment, National Institute for Physiological Sciences.

⊥ Department of Chemistry, University of Tokyo.

Department of Informational Physiology, National Institute for Physiological Sciences.

[1] Abbreviations: VDSC, voltage-dependent sodium channel; CaM, calmodulin; SD medium, minimal synthetic dropout medium; CD, circular dichroism; ESI-MS, electrospray-ionization mass spectrometry; PAGE, polyacrylamide gel electrophoresis; Hepes, 4-(2-hydroxyethyl)-1-piperazineethanesulfonic acid; Tris, tris(hydroxymethyl)aminomethane; EGTA, ethylene glycol bis(β-aminoethyl ether)-*N*,*N*,*N*′,*N*′-tetraacetic acid.

10.1021/bi9912600 CCC: $19.00
Published on Web 01/20/2000

VDSC, and the consequent Ca^{2+}-dependent structural transition of the complex.

MATERIALS AND METHODS

Materials

Hepes, dansyl chloride, and EGTA of the highest purity grade were obtained from Sigma Chemical Co. Dr. M. Noda (National Institute for Basic Biology, Japan) kindly provided the rat brain VDSC type II cDNA (*18*). Two synthetic peptides, NaIQ and NaBaa (Figure 1B), derived from the VDSC sequence (*2*), were obtained from Bio-Synthesis Inc. The peptides were purified by high-performance liquid chromatography and verified by mass spectrometry.

Methods

Two-Hybrid Screening. Yeast two-hybrid screening was done using Matchmaker Two-Hybrid System 2 (Clontech). Bait was constructed in the plasmid pAS2-1C (provided by Dr. T. Maeda, University of Tokyo, Japan), which carries the cDNA sequence that encodes the Gal4 DNA binding domain. Plasmid pAS2-1C was constructed by replacing the 2 μm origin of pAS2-1 (Clontech) with the *CEN-ARS* origin (*19*). The efficiency of Y190 yeast cell transformation with pAS2-1C was 10 times higher than that with the original pAS2-1. The VDSC cDNA fragment encoding the C-terminal domain of rat brain VDSC type II was amplified by PCR using HF DNA polymerase (Boehringer Mannheim) with the following primers:

sense primer:
5′-CGCCATATGGAGAATTCACGTCGCC-3′

antisense primer:
5′-CGCCTGCAGTTACTTTTTACTTTCCCTGAT-3′

The amplified cDNA fragment (encoding amino acid residues 1777−2005; see ref *2*) was inserted into the *Nde*I−*Pst*I site of pAS2-1C to yield bait plasmid pGal4VDSCC1. The nucleotide sequence of the bait construct was confirmed by the dye terminator method. The two-hybrid screening and the interaction assay were performed essentially as described in the Matchmaker 2 protocol (Clontech). Strain Y190 yeast cells containing *LacZ* and *His3* reporter genes with upstream *Gal4* operators were transformed with bait plasmid pGal4VDSCC1. Y190 cells containing the bait plasmid were retransformed with a rat brain cDNA library (Clontech) by a lithium acetate method. Transformants were plated on minimal medium lacking leucine, tryptophan, and histidine in the presence of 25 mM 3-amino-1,2,4-triazole (SD/−Leu/−Trp/−His/+25 mM 3-AT) and incubated for 7 days at 30 °C. This yielded 5.5×10^6 Leu^+ and Trp^+ transformants (2×10^5/μg of DNA). β-Galactosidase assay of His^+ cells was conducted as described in the Matchmaker 2 protocol.

Two-Hybrid Interaction Assay of the VDSC C-Terminal Domain with CaM. The cDNA fragment encoding the VDSC C-terminal domain was mutated by PCR to obtain deleted or truncated mutants. These cDNA fragments were introduced into pAS2-1C to yield mutant bait plasmids pGal4VDSCC2 (encoding amino acid residues 1777−1938), pGal4VDSCC3 (1777−1900), pGal4VDSCC4 (1866−2005), and pGal4VDSCC5 (1777−1900 and 1939−2005) (Figure 1A). The nucleotide sequences of the bait constructs were confirmed by the dye terminator method. One of the mutant bait plasmids and the plasmid encoding rat CaM (pRCaM), identified through the yeast two-hybrid screening, were cotransfected into Y190 cells. Transformants were plated onto SD/−Leu/−Trp/−His/+25 mM 3-AT plates and incubated for 5 days at 30 °C. Reporter gene *LacZ* activity was studied using β-galactosidase assay as described in the Matchmaker 2 protocol.

Fusion Proteins. Expression plasmids for two S-Tag fusion proteins were constructed in pET32a (Novagen). Plasmid pETfull contained the cDNA sequence encoding the entire C-terminal domain (amino acid residues 1777−2005), and plasmid pETΔRegion 2 contained the cDNA insert encoding amino acid residues 1777−1900 and 1939−2005 (missing Region 2). Bacterial cells of *E. coli* BL21(DE3)pLysS (*20*) were transfected by each plasmid, and two fusion proteins were expressed as described in the protocol (Novagen). To purify fusion proteins, bacterial lysates were applied to nickel−Sepharose columns. Eluted fractions were checked for purity by Coomassie brilliant blue staining of SDS−PAGE. Purified fusion proteins were digested with thrombin to remove the thioredoxin and His-tag region.

Pull-Down Assay. Mixtures of rat brain extracts [100 μg of protein in total volume (1 mL)], each fusion protein (10 μg of protein in total volume), and S-protein agarose (Novagen; 50 μL in total volume) that specifically binds to S-tag of fusion proteins (*21*) were incubated for 30 min at 4 °C in the following solutions: 50 mM Hepes/Tris (pH 7.3), 150 mM KCl, and 1% Nonidet P-40 in the presence (0.5 mM $CaCl_2$: buffer A) or absence (2 mM EGTA: buffer B) of Ca^{2+}. Mixtures were then washed 5 times with buffer A or B (1 mL × 5). After brief centrifugation, proteins bound to the agarose were eluted with SDS−PAGE sample buffer (50 μL), and 15 μL of each sample was applied to a 12.5% gel. After electrophoresis, the gel was electroblotted onto a nitrocellulose membrane. CaM was detected by an anti-CaM monoclonal antibody (Upstate Biotechnology) and alkaline phosphatase-linked secondary antibody (Bio-Rad), and visualized by chemiluminescence (NEN).

Gel Mobility Shift Assay. Different concentrations of peptides derived from VDSC (NaIQ and NaBaa) were incubated with 2 μM CaM (purified as ref *22*), in 30 mM Hepes/Tris, pH 7.3, 150 mM KCl, 0.1% Nonidet P-40, and 1 mM $CaCl_2$ or 2 mM EGTA for 30 min at room temperature. These mixtures were loaded on nondenaturing 12.5% polyacrylamide gels containing 1 mM $CaCl_2$ or 2 mM EGTA and visualized by silver staining.

CaM Dansylation. Fluorescent dansylated CaM (dansyl-CaM) was prepared using rat brain CaM and dansyl chloride as described previously (*23*). Additionally, the dialyzed mixture of dansyl chloride with CaM was applied to a PD-10 column (Sephadex-25G, Pharmacia) to remove remaining free dansyl chloride. Measurement of the absorbance at 320 nm using a molar extinction coefficient of 3400 M^{-1} cm^{-1} (*24*) showed incorporation of about 0.6 mol of dansyl moiety/mol of CaM.

Fluorescence Spectroscopy. Fluorescence spectra were recorded in a quartz cuvette (light path: 10 mm), using a Hitachi F-4500 fluorescent photometer. Each peptide dissolved in distilled water was added to a cuvette containing

dansyl-CaM. The concentration of dansyl-CaM was 120 nM in 30 mM Hepes/Tris (pH 7.3), 150 mM KCl, and 1 mM $CaCl_2$ or 2 mM EGTA. To ensure equilibration of the mixture, the sample was constantly stirred for 15 min at 25 °C before measurement. The excitation wavelength (Ex) was 340 nm, the measured emission wavelength (Em) was 400−600 nm, and both excitation and emission bandwidths were 10 nm. The fluorescence spectrum for each sample is an average of five scans. For the titration experiments, the fluorescence intensity was measured at Em 480 nm integrated for 5 s for each sample. The binding model used to fit the dansyl fluorescence data was simply

$$\text{pep} + \text{CaM} \leftrightarrow \text{pep·CaM}$$

where pep is the peptide (NaBaa or NaIQ) and pep·CaM the peptide−CaM complex. The dissociation constant K_d is

$$K_d = \frac{([\text{CaM}]_0 - [\text{pep·CaM}])([\text{pep}]_0 - [\text{pep·CaM}])}{[\text{pep·CaM}]} \quad (1)$$

where $[\text{CaM}]_0$ is the initial concentration of CaM and $[\text{pep}]_0$ that of the peptide. Fluorescence intensity is assumed to be a linear function of [pep·CaM]:

$$F_{480} = F_b[\text{pep·CaM}] + F_0 \quad (2)$$

Experimental fluorescence data given as a function of $[\text{pep}]_0$ were fitted by combining eqs 1 and 2 using a nonlinear least-squares program (*25*) run on a personal computer. Fitting parameters were F_b, F_0, and K_d.

Ca^{2+} Dependence of Fluorescence. Fluorescence intensity was obtained at Em 480 in 30 mM Hepes/Tris, pH 7.3, 150 mM KCl, and 2 mM EGTA buffer containing 120 nM dansyl-CaM and 250 nM NaIQ or 800 nM NaBaa, with an increasing concentration of Ca^{2+}. Free Ca^{2+} concentration was calculated according to ref *26*. Relative fluorescence was calculated by the following equation: relative fluorescence $= (F - F_0)/(F_{max} - F_0)$, where F is the measured intensity, F_{max} is the maximum intensity, and F_0 is the intensity without added Ca^{2+}.

Identification of Dansylated Site in Dansyl-CaM. The molecular weights of CaM and dansyl-CaM were determined by an electrospray-ionization mass spectrometer, ESI-MS API-300 (Perkin-Elmer), to calculate the number of dansylated sites in a dansyl-CaM molecule. To identify the specific dansylation site, CaM and dansyl-CaM (50 μg of each) were digested by trypsin (Sigma) in 20 mM Tris/pH 8.0 with HCl, 100 mM NaCl, 1 mM $CaCl_2$, 2 M urea, and 1% CaM or dansyl-CaM for 4 h at room temperature. Tryptic peptides were separated out using a SMART system with a μRPC C2/C18 column (Pharmacia). The mobile phase was 0.1% trifluoroacetic acid and an increasing gradient of 0−50% acetonitrile for 50 min at room temperature. Separated fractions were lyophilized and dissolved in distilled water (total volume: 200 μL). Lyophilized fractions were measured for the fluorescence by a fluorescence micro-plate reader, MTP-100F (Corona Electric), with Ex 360 nm and Em 500 nm. Only one specific fraction of the dansyl-CaM products showed strong fluorescence emission, and the peptide sequence of the fraction was determined by the Edman method. Automated sequence analysis was conducted using an ABI494 protein sequencer (Applied Biosystem), and phenylthiohydantoin derivatives of amino acids were identified by reverse-phase high-performance liquid chromatography.

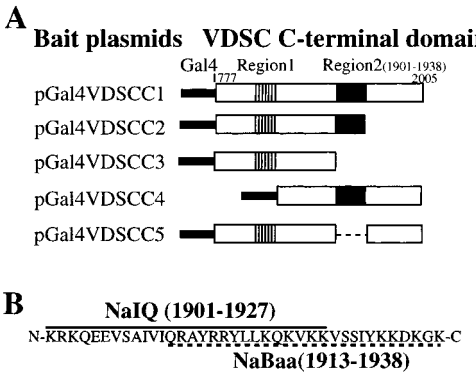

FIGURE 1: (A) Constructs for wild-type and mutated VDSC C-terminal domains used in the two-hybrid interaction assay. The Gal4 sequence (thick solid line) was fused with the wild-type or deleted sequences encoding the C-terminal domain (boxes). Putative CaM binding sites, Region 1 and Region 2, are indicated by striped and dark shaded boxes, respectively. The dashed line indicates deletion of Region 2. (B) Amino acid sequence of synthetic peptides (NaIQ and NaBaa). Region 2 corresponds to amino acid residues 1901−1938 of type II VDSC. The solid line above the sequence indicates NaIQ, the dashed line under the sequence NaBaa.

Circular Dichroism Spectroscopy. Circular dichroism (CD) spectra were measured with a J-720WI spectropolarimeter (Jasco) using a quartz cuvette with a light path of 2 mm at 25 °C in 30 mM Hepes/Tris, pH 7.3, 150 mM KCl, and 0.5 mM $CaCl_2$ or 5 mM EGTA. Spectra were obtained by scanning at 100 nm/min over a wavelength range of 190−250 nm. Far-UV CD spectra were measured at 10 μM peptide and 5 μM CaM. For each sample, 16 scans were averaged. Mean residue ellipticity, $[\theta]$, was determined from the relationship: $[\theta] = \theta/10cdr$, where θ is the ellipticity in degrees, c the protein concentration (M), d the path length (cm), and r the number of amino acid residues (148 in the case of CaM). The ellipticity of the mixture was obtained by subtracting the record of the peptide alone measured in advance.

RESULTS

Two-Hybrid Screening. To search for proteins that interact with the C-terminal domain of VDSC type II (*2*), we used yeast two-hybrid screening of an expression cDNA library from rat brain with 5.5×10^6 independent clones, and obtained 20 positive colonies. Four of the positive clones carried full-length rat calmodulin (CaM) cDNA (*27*) (plasmid: pRCaM). The remainder of the positive clones were found to encode only short peptides (10−15 amino acid residues) fused with the Gal4 activation domain, and were not studied further.

Two-Hybrid Interaction Assay. Reports on CaM binding proteins have shown that CaM binds to several consensus sequence motifs, such as the Baa motif (*b*asic *a*mphipathic α-helix) (*28*) and the IQ motif (IQXXXRGXXXR, where X is any amino acid) (*29*, *30*). We searched for these types of CaM binding motifs in the VDSC C-terminal domain to find two candidate regions for CaM binding (designated Region 1 and Region 2; Figure 1A). Region 1 (amino acid residues 1852−1866) has a Baa motif, whereas Region 2 (1919−1933) has both Baa and IQ-like motifs (Figure 1B).

Table 1: Two-Hybrid Interaction Assay between Mutated C-Terminal Domains and CaM

bait plasmid/pray plasmid	cell growth[a]	LacZ activity[b]
pGalVDSCC1/−	−	−
−/pRCaM	−	−
pGalVDSCC1/pRCaM	++	++
pGalVDSCC2/pRCaM	+++	+++
pGalVDSCC3/pRCaM	+	−
pGalVDSCC4/pRCaM	++	++
pGalVDSCC5/pRCaM	−	−

[a] Growth of yeast incubated 5 days after cotransfection. [b] LacZ activity studied using β-galactosidase assay: (−) none, (+) weak, (++) moderate, and (+++) strong.

To determine whether Region 1 and Region 2 are actual CaM binding regions, we performed a two-hybrid interaction assay using four mutated C-terminal domains of the VDSC α-subunit as bait proteins (Figure 1A). Y190 cells were cotransfected with pRCaM and one of the bait plasmids. Y190 cells cotransfected with pRCaM and pGal4VDSCC5 (containing Region 1 but not Region 2) did not grow on selection plates (Table 1). Cells cotransfected with pRCaM and pGal4VDSCC3 (containing Region 1 but not Region 2 and the following residues) grew feebly on selection plates, but β-galactosidase activity was not detected. In contrast, cells cotransfected with pRCaM and one of the pGal4VDSCC1, -2, or -4 (all containing Region 2) showed moderate or high β-galactosidase activity. The results of the two-hybrid interaction assay indicate that Region 2 is a CaM binding region in the VDSC C-terminal domain in the yeast two-hybrid system.

Pull-Down Assay. Ca^{2+} dependence of CaM binding to its target proteins is the critical property that controls the binding process. However, in the yeast two-hybrid system, it is difficult to determine whether the CaM molecule is Ca^{2+}-free apoCaM or Ca^{2+}-bound Ca^{2+}CaM because this system detects molecular interaction in an intranuclear environment (*6*). We studied the Ca^{2+} dependence of binding between Region 2 and CaM using a pull-down assay. Two fusion proteins, one carrying the full-length C-terminal protein (Full-length) and the other having the C-terminal domain without Region 2 (ΔRegion 2), were bound to S-protein agarose, and purified CaM was adsorbed to the fusion protein−agarose complex. Immunoblot analysis using an anti-CaM antibody showed that CaM was detected only in the mixture of CaM and the agarose containing Full-length, either in the presence or in the absence of Ca^{2+}, but not in mixtures containing ΔRegion 2 or the control S-protein (Figure 2). Binding of CaM with Full-length fusion protein was even stronger in the absence of Ca^{2+} than in the presence of Ca^{2+}.

Gel Mobility Shift Assay. Region 2 contains both IQ-like and Baa motifs. We prepared two synthetic peptides, NaIQ and NaBaa, whose sequences contain IQ-like or Baa motifs (Figure 1B). We then analyzed the binding properties between the peptides and CaM in a gel mobility shift assay. In the presence of Ca^{2+}, CaM preincubation with either NaIQ or NaBaa delayed the mobility of the CaM band (Figure 3A,C). Mixtures of higher ratios of either peptide to CaM showed a larger population of the slowly mobile CaM band. A complete shift of the mobility occurred at a peptide to CaM ratio of 4:1 for NaIQ (Figure 3A), while NaBaa caused no complete shift under our experimental conditions (Figure 3C). Thus, in the presence of Ca^{2+}, CaM was able to bind to both peptides with a higher affinity for NaIQ than for NaBaa (compare Figure 3A and Figure 3C). In the absence of Ca^{2+} (2 mM EGTA), no band shift was observed for the mixture of NaBaa and CaM (Figure 3D), whereas the NaIQ and CaM mixture still strongly delayed CaM band mobility (Figure 3B). A complete shift occurred at an NaIQ:CaM molar ratio of 2:1. The results demonstrated that whereas the interaction between the Baa motif and CaM is Ca^{2+}-dependent, the IQ-like motif of VDSC can bind to CaM in a Ca^{2+}-independent manner.

Fluorescence Spectroscopy. Binding of the two peptides with CaM was also studied using dansylated CaM (dansyl-CaM). Dansyl-CaM is a useful tool to detect interactions between CaM and other proteins and conformational changes of CaM, because the fluorescence spectrum is shifted and the intensity is enhanced when the environment of the dansyl moiety becomes hydrophobic (*31*). In the presence of Ca^{2+}, the blue shift and enhancement of the dansyl fluorescence

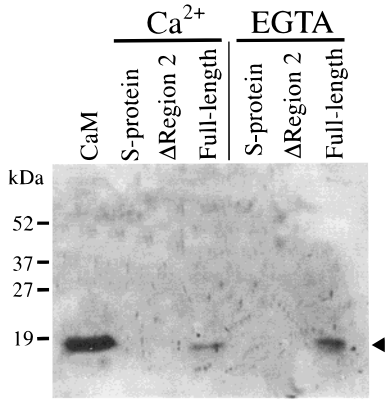

FIGURE 2: Pull-down assay. The full-length fusion protein of the C-terminal domain (Full-length) or the Region 2-deletion fusion protein (ΔRegion 2) (10 μg of each) was incubated with S-protein agarose (50 μL) and rat brain extracts (100 μg of protein) in the presence of Ca^{2+} (0.5 mM) or EGTA (2 mM). The "S-protein" did not contain fusion proteins in the mixture. After washing by brief centrifugation, the pellet was solubilized with 50 μL of a SDS−PAGE sample buffer. CaM was detected by immunoblot analysis using an anti-CaM monoclonal antibody. CaM (10 ng) was run as a control.

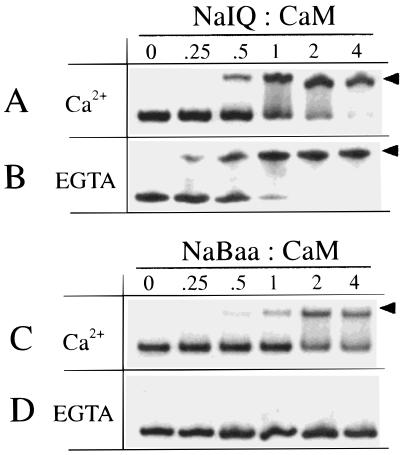

FIGURE 3: Gel mobility shift assay. CaM (2 μM) was incubated with NaIQ (A, B) or NaBaa (C, D) at different molar ratios in the presence of Ca^{2+} (1 mM $CaCl_2$; A, C) or in the absence of Ca^{2+} (2 mM EGTA; B, D). Each gel was visualized by silver staining. Arrowheads indicate the band of the peptide·CaM complex.

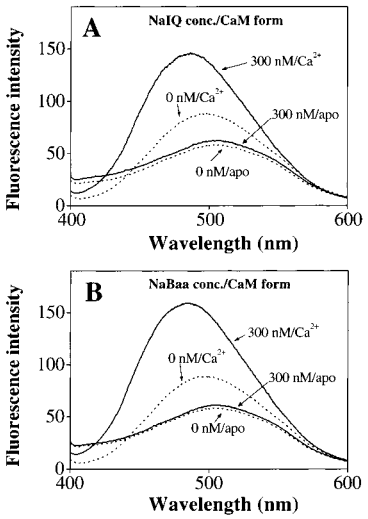

FIGURE 4: Changes in the dansyl-CaM fluorescence spectrum induced by peptides NaIQ (A) and NaBaa (B). Emission spectrum of dansyl-CaM (120 nM) alone (dotted lines), and mixtures of dansyl-CaM (120 nM) and peptides (300 nM) (solid lines) in the presence or absence of Ca^{2+}. Peptide concentration and CaM form are indicated for each line.

Table 2: Summary of the Results on Peptide−CaM Binding

peptide−CaM	gel mobility shift assay[a] peptide:CaM	fluorescence spectroscopy[b] K_d	fluorescence spectroscopy[b] increment (480 nm)	CD spectroscopy[c] increment (222 nm)
NaIQ−Ca^{2+}CaM	4:1	5 nM	93%	enhanced
NaBaa−Ca^{2+}CaM	<4:1	90 nM	114%	nd
NaIQ−apoCaM	2:1	nd	7%	enhanced
NaBaa−apoCaM	no shift	nd	3%	nd

[a] Peptide-to-CaM ratio where complete shift was observed. "No shift" indicates that no complex was detected. [b] Dissociation constants (K_d) of peptides for CaM and increments of fluorescence intensity (480 nm) induced by peptides. [c] Changes in negative ellipticity induced by peptides. nd = not determined.

spectrum were observed when 300 nM NaIQ peptide or NaBaa peptide was added (Figure 4). To quantitate binding analysis, we applied peptide titration. Apparent dissociation constants (K_d) obtained by fitting experimental results using a nonlinear least-squares program were 5 nM for NaIQ·dansyl-Ca^{2+}CaM and 90 nM for NaBaa·dansyl-Ca^{2+}CaM (Table 2), suggesting that Region 2 of VDSC contains two CaM binding sites with different affinities to CaM.

In the absence of Ca^{2+}, as suggested from the result of the gel mobility shift assay, NaBaa did not alter the fluorescence spectrum, confirming that NaBaa does not bind to dansyl-CaM (Figure 4B). Surprisingly, addition of 300 nM NaIQ failed to affect the fluorescence spectrum (Figure 4A), although the results of the gel mobility shift assay described above unambiguously indicated that NaIQ binds to apoCaM (Figure 3). To solve this apparent discrepancy, we conducted a series of experiments. We first determined the number of dansylated sites in a dansyl-CaM molecule using ESI-MS. Comparison of the molecular weights of CaM and dansyl-CaM indicated that dansyl-CaM contains a single dansyl moiety (data not shown). We then identified Lys_{75} as the dansylated site by determining the amino acid sequence of the fluorescent tryptic peptide (data not shown), consistent with the previous report (*32*). Lys_{75} is located near the flexible linker (amino acid residues 77−80) which connects

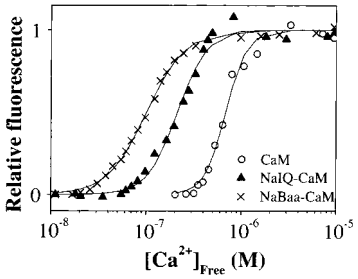

FIGURE 5: Ca^{2+} dependency of dansyl-CaM fluorescence with or without peptides. Normalized fluorescence is shown for CaM (○), NaIQ−CaM mixture (▲), and NaBaa−CaM mixture (×) under assay conditions described under Materials and Methods. Sigmoidal curves are just for visualization.

the N- and C-terminal globular Ca^{2+} binding domains of CaM (*33*, *34*). Third, we tested the effect of dansylation on the gel mobility shift assay. We used dansyl-CaM instead of CaM to obtain the same band shift in the absence of Ca^{2+} (data not shown). This result indicates that NaIQ can bind to dansyl-CaM Ca^{2+}-independently to form the NaIQ·dansyl-CaM complex, excluding the possibility that addition of the dansyl moiety prevents NaIQ from binding to CaM. Taken together, although NaIQ and dansyl-CaM bind in the presence and absence of Ca^{2+}, the binding in the presence of Ca^{2+} alters the fluorescence spectrum, whereas the binding in the absence of Ca^{2+} cannot be detected by spectroscopy, indicating that the NaIQ−CaM complex has two conformational states, interchanging Ca^{2+} dependently.

To analyze the Ca^{2+} dependency of the conformational states, we applied Ca^{2+} titration (Figure 5). Without peptides, dansyl-CaM exhibited fluorescence changes in a Ca^{2+} concentration range of 0.5−2 μM. The fluorescence changes of the NaBaa·dansyl-CaM complex occurred in a much lower Ca^{2+} concentration range, which may correspond to a physiological Ca^{2+} concentration. The NaIQ·dansyl-CaM complex showed an intermediate Ca^{2+} dependency.

CD Spectroscopy. Protein−protein interaction can be detected by the conformational analysis of proteins. Far-UV CD spectroscopy is a powerful tool for detecting changes in the secondary structure of CaM induced by binding with peptides (*35*). The CD spectral measurements were performed here to detect conformational changes accompanied by the formation of the NaIQ·CaM complexes. The bee venom peptide melittin (peptide of 26 amino acid residues) was used as a control. Melittin binds to CaM with a very high affinity in a Ca^{2+}-dependent manner (*36*, *37*). In the presence of Ca^{2+}, the spectrum of the NaIQ−Ca^{2+}CaM mixture showed enhanced negative ellipticity compared to the spectrum of Ca^{2+}CaM alone (Figure 6A), indicating that the NaIQ·Ca^{2+}CaM complex shows a significant increase in α-helical content upon complex formation.

In the absence of Ca^{2+}, the melittin−apoCaM mixture showed a marginal increase in α-helical content, as expected from little binding of melittin to CaM in the Ca^{2+}-free condition (Figure 6B). In contrast, the NaIQ−apoCaM mixture showed significantly enhanced negative ellipticity at around 222 nm (Figure 6B), indicating that NaIQ binds to apoCaM even in the absence of Ca^{2+}, and that the α-helical structure was induced upon formation of the NaIQ·apoCaM complex. Furthermore, the spectra of the NaIQ·

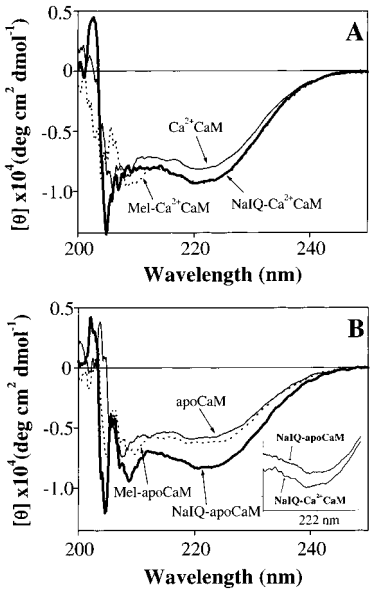

FIGURE 6: CD spectra of CaM and peptide−CaM mixtures. CD spectra of CaM alone (thin solid lines), NaIQ−CaM mixture (thick solid lines), and melittin−CaM mixture (dotted lines) in the presence (A) or absence (B) of Ca^{2+}. Inset in panel B: CD spectra around 222 nm of NaIQ−Ca^{2+}CaM and NaIQ−apoCaM. The vertical and horizontal axes are on the same scale in panels A and B, and the inset.

Ca^{2+}CaM and NaIQ·apoCaM complexes were slightly but significantly different (Figure 6B, inset). Because the helical change in CaM conformation (without peptide) induced by Ca^{2+} has reported about 11 amino acid residues (*38*, *39*), a simple estimate suggests that the spectral amplitude from NaIQ·apoCaM to NaIQ·Ca^{2+}CaM (ca. 40% without peptide) corresponds to the formation of α-helix of four to five residues. The α-helix inducible site of CaM is speculated under Discussion.

DISCUSSION

Complex Formation of CaM and VDSC. We have discovered that the Ca^{2+} binding protein CaM directly binds to the α-subunit of VDSC. CaM is known to bind to a wide range of functional proteins (*7*), and several consensus motifs for CaM binding have been proposed. We found two regions which contain the consensus motifs in the C-terminal domain of VDSC. The yeast two-hybrid interaction assay confirmed one of the two regions as an actual CaM binding site. The identified region, Region 2, contains the sequences of both Baa and IQ-like motifs for CaM binding. The Baa motif (basic amphipathic α-helix) of 15−20 residues has been found in several CaM binding proteins and peptides, such as melittin (*36*, *37*), CaMKII (*40*), and MLCK (*41*). They bind to CaM Ca^{2+}-dependently. The IQ motif (IQXXXRGXXXR) of 11 residues is another CaM binding motif, found in proteins such as growth cone associated protein 43 kDa (GAP-43/neuromodulin) (*42*, *43*), CNG channel β-subunit (*10, 11*), and L-type VDCC (*17, 18*) (Table 3). IQ motif proteins have more diverse Ca^{2+} sensitivity than Baa motif proteins. Some IQ motif proteins such as neuromodulin or neurogranin bind CaM preferentially in the absence of Ca^{2+} (*42*−*44*), some proteins only in the presence of Ca^{2+} (*17* and *18*), and other proteins Ca^{2+}-independently (*45*). In this work, we showed that the VDSC C-terminal domain binds not only to Ca^{2+}-bound Ca^{2+}CaM but also to Ca^{2+}-free apoCaM. CaM is well-known to be one of the primary Ca^{2+} sensors, regulating the activity of many target proteins when Ca^{2+} binds to CaM (*7*). Nevertheless, the physiological significance of the Ca^{2+}-independent binding or the relationship between the Ca^{2+}-dependent and Ca^{2+}-independent binding has not been studied well. In the present case, Region 2 in the VDSC C-terminal domain presents such an interesting model of CaM binding, in which both Ca^{2+}-dependent and Ca^{2+}-independent interactions are involved.

Table 3: Alignment of the IQ-like Motif in the C-Terminal of VDSC Type II with Other VDSC Proteins and CaM Binding Proteins Containing IQ Motifs[a]

VDSC type II	(rat)	KRKQEEVSAIVIQRAYRRYLLKQKVKK
VDSC type III	(rat)	EVSAAIIQRNYRCYLLKQRLKNI
VDSC rPN4	(rat)	EVSAVVLQRAYRGHLARRGFICR
L-type VDCC	(human)	KFYATFLIQEYFRKFKKRKEQ
CNG β-subunit	(bovine)	AIINDLQELVKLFKERTEKVKEKLI
Myosin I	(Chicken)	EALATLIQKMFRGWCCRKRYQ
GAP-43	(human)	AHKAATKIQASFRGHITRKKLKDE

[a] Boldface and shaded characters indicate the IQ motif consensus sequence. Underlined and shaded characters indicate residues homologous to the consensus sequence. VDSC type III (*50*), rPN4 (*51*), L-type VDCC (*16*), CNG β-subunit (*11*), myosin I (*29*), GAP-43 (*44*).

Binding Site and Structure of NaIQ·CaM in the Presence and Absence of Ca^{2+}. We examined the CaM binding properties of Region 2 using two synthetic peptides, NaIQ and NaBaa. Table 2 summarizes the results from three different series of experiments. While half of the residues (15 aa) of the NaIQ and NaBaa sequences are overlapped, the two peptides exhibit distinct Ca^{2+} dependency of CaM binding; NaBaa binds to CaM Ca^{2+}-dependently, and NaIQ binds to CaM Ca^{2+}-independently. Thus, the NaBaa sequence is sufficient for Ca^{2+}CaM binding but not for apoCaM binding, whereas the NaIQ sequence is essential for apoCaM binding. This observation suggests that the binding sites for apoCaM and Ca^{2+}CaM are not identical.

Although NaIQ binds to CaM in a Ca^{2+}-independent manner, the fluorescence spectrum of NaIQ−dansyl-CaM was found to depend on the Ca^{2+} concentration in the solution. Together with several supplementary experiments, we concluded that the conformation of the NaIQ·CaM complex is different, depending on Ca^{2+} concentration (see Results). Without peptides, the state transition from apoCaM to Ca^{2+}CaM on addition of Ca^{2+} alters the fluorescence spectrum of dansyl-CaM. This change is caused by an α-helix formation of the flexible linker domain (consisting of 4 residues) in the close vicinity of which Lys_{75} resides (*39*). In the presence of Ca^{2+}, addition of NaIQ results in a more pronounced blue shift and a greater enhancement of the fluorescence, indicating that NaIQ binding greatly alters the environment in the vicinity of dansylated Lys_{75}. Direct contact of the peptide to Lys_{75} (*46*) and more global conformational changes of CaM induced by peptide binding (*46*, *47*) would cause the fluorescence changes. In the absence of Ca^{2+}, however, the fluorescence spectrum of NaIQ−apoCaM was practically identical to that of apoCaM, suggesting that NaIQ binds to apoCaM at a site away from

Lys_{75}, and that the CaM flexible linker conformation was not affected on NaIQ binding. The notion that NaIQ binds to CaM at different sites Ca^{2+}-dependently is supported by the nuclear magnetic resonance study on the interaction between the IQ motif peptide "Neurop" derived from neuromodulin and apoCaM, which showed that the Neurop peptide binds to the C-terminal domain of CaM, but not to the flexible linker domain (*48*). As for the conformational difference of the peptide·CaM complex, our results of CD spectroscopy that a stretch of four to five residues forms an α-helix in the state transition from NaIQ·apoCaM to NaIQ·Ca^{2+}CaM provide further supporting evidence that CaM is in different conformational states depending on Ca^{2+}. Thus, NaIQ·apoCaM and NaIQ·Ca^{2+}CaM are in two conformational states, distinct with respect to the peptide binding site and the CaM conformation.

The Ca^{2+} titration experiments in Figure 5 for CaM alone, NaBaa−CaM, and NaIQ−CaM provide information about the conformational transitions:

$$\mathrm{CaM} + n\mathrm{Ca}^{2+} \rightarrow \mathrm{CaM}\cdot n\mathrm{Ca}^{2+}$$

$$\mathrm{NaBaa} + \mathrm{CaM} + n\mathrm{Ca}^{2+} \rightarrow \mathrm{NaBaa}\cdot\mathrm{CaM}\cdot n\mathrm{Ca}^{2+}$$

$$\mathrm{NaIQ}\cdot\mathrm{CaM} + n\mathrm{Ca}^{2+} \rightarrow \mathrm{NaIQ}\cdot\mathrm{CaM}\cdot n\mathrm{Ca}^{2+}$$

The results that peptide·CaM complexes bind with Ca^{2+} at lower Ca^{2+} concentrations than CaM indicate that the peptide binding to CaM enhances the Ca^{2+} affinity of CaM. This implies that the binding of VDSC to CaM increases the Ca^{2+} sensitivity of CaM, which in turn couples with the conformational transition of the CaM·VDSC complex.

What Is the Function of the CaM·VDSC Complex? High-affinity CaM-target proteins ($K_d \leq 10$ nM) are thought to be activated efficiently throughout mammalian cells (*49*). In our results, K_d is 5 nM for NaIQ·Ca^{2+}CaM. We assume that this value is sufficiently small enough to cause functional interactions between CaM and VDSC in neuronal cells. The Ca^{2+} concentration where the state transition between NaIQ·apoCaM and NaIQ·Ca^{2+}CaM is halfway is 250 nM in the Ca^{2+} titration experiment (Figure 5, triangles). This concentration is higher than the basal Ca^{2+} level (about 100 nM), but is an easily attainable level when a train of action potentials are generated. In response to changes in intracellular Ca^{2+} concentration, the complex conformation will shift from apoCaM·VDSC to Ca^{2+}CaM·VDSC, and vice versa. Recent observations showed that functions of several ion channels are modulated by direct binding of CaM, which acts as a Ca^{2+} sensor. Besides the Ca^{2+}-dependent binding, CaM is concentrated in nerve terminals through the apoCaM·GAP43 interaction in neuronal cells (*43*). In a similar way, interaction of CaM with the IQ-like motif in VDSC may be required to keep a sufficient CaM concentration in low-Ca^{2+} conditions. Although the functional significance of apoCaM or Ca^{2+}CaM binding has not been elucidated for VDSC, the amino acid sequences around Region 2 are well conserved among the VDSC α-subunits (Table 3), suggesting that regulation through CaM binding may be a common mechanism for VDSC. Future work should be directed to study the in vivo binding of CaM to VDSC and the functional significance of CaM binding in neurons.

ACKNOWLEDGMENT

We thank Dr. M. Noda for providing the voltage-dependent sodium channel type II cDNA, Dr. T. Maeda for providing pAS2-1C plasmid, and Ms. Y. Makino (National Institute for Basic Biology, Center for Analytical Instruments) for operating the mass spectrometer and the protein sequencer.

REFERENCES

1. Catterall, W. A. (1995) *Annu. Rev. Biochem. 64*, 493−531.
2. Noda, M., Ikeda, T., Kayano, T., Suzuki, H., Takeshima, H., Kurasaki, M., Takahashi, H., and Numa, S. (1986) *Nature 320*, 188−192.
3. Ma, J. Y., Catterall, W. A., and Scheuer, T. (1997) *Neuron 19*, 443−452.
4. Srinivasan, Y., Elmer, L., Davis, J., Bennett, V., and Angelides, K. (1988) *Nature 333*, 177−180.
5. Tibbs, V. C., Gray, P. C., Catterall, W. A., and Murphy, B. J. (1998) *J. Biol. Chem. 273*, 25783−25788.
6. Fields, S., and Song, O. (1989) *Nature 340*, 245−246.
7. Nelson, M. R., and Chazin, W. J. (1998) in *Calmodulin and Signal Transduction* (Van Eldik, L. J., and Watterson, D. M., Eds.) pp 17−64, Academic Press, San Diego, CA.
8. Saimi, Y., and Ling, K. Y. (1990) *Science 249*, 1441−1444.
9. Saimi, Y., and Kung, C. (1994) *FEBS Lett. 350*, 155−158.
10. Grunwald, M. E., Yu, W. P., Yu, H. H., and Yau, K. W. (1998) *J. Biol. Chem. 273*, 9148−9157.
11. Weitz, D., Zoche, M., Muller, F., Beyermann, M., Korschen, H. G., Kaupp, U. B., and Koch, K. W. (1998) *EMBO J. 17*, 2273−2284.
12. Ehlers, M. D., Zhang, S., Bernhadt, J. P., and Huganir, R. L. (1996) *Cell 84*, 745−755.
13. Xia, X. M., Fakler, B., Rivard, A., Wayman, G., Johnson-Pais, T., Keen, J. E., Ishii, T., Hirschberg, B., Bond, C. T., Lutsenko, S., Maylie, J., and Adelman, J. P. (1998) *Nature 395*, 503−507.
14. Qin, N., Olcese, R., Bransby, M., Lin, T., and Birnbaumer, L. (1999) *Proc. Natl. Acad. Sci. U.S.A. 96*, 2435−2438.
15. Peterson, B. Z., DeMaria, C. D., and Yue, D. T. (1999) *Neuron 22*, 549−558.
16. Zühlke, R. D., Pitt, G. S., Deissseroth, K., Tsein, R. W., and Reuter, H. (1999) *Nature 399*, 159−162.
17. Lee, A., Wong, S. T., Gallagher, D., Li, B., Storm, D. R., Scheuer, T., and Catterall, W. A. (1999) *Nature 399*, 155−159.
18. Stühmer, W., Conti, F., Suzuki, H., Wang, X. D., Noda, M., Yahagi, N., Kubo, H., and Numa, S. (1989) *Nature 339*, 597−603.
19. Shinobu, N., Maeda, T., Aso, T., Ito, T., Kondo, T., Koike, K., and Hatakeyama, M. (1999) *J. Biol. Chem. 274*, 17003−17010.
20. Studier, F. W. (1991) *J. Mol. Biol. 219*, 37−44.
21. LaVallie, E. R., DiBlasio, E. A., Kovacic, S., Grant, K. L., Schendel, P. F., and McCoy, J. M. (1993) *Bio/Technology 11*, 187−193.
22. Gopalakrishna, R., and Anderson, W. B. (1982) *Biochem. Biophys. Res. Commun. 104*, 830−836.
23. Vorherr, T., James, P., Krebs, J., Enyedi, A., McCormick, D. J., Penniston, J. T., and Carafoli, E. (1990) *Biochemistry 29*, 355−365.
24. Chen, R. F. (1968) *Anal. Biochem. 25*, 412−416.
25. Press, W. H., Flanney, B. P., Teukolsky, S. A., and Vetterling, W. T. (1988) *Numerical Recipes in C*, Cambridge University Press, Cambridge, U.K.
26. Schwarzenbach, G., Senn, H., and Anderegg, G. (1957) *Helv. Chim. Acta 40*, 1886−1900.
27. Dedman, J. R., Jackson, R. L., Schreiber, W. E., and Means, A. R. (1978) *J. Biol. Chem. 253*, 343−346.
28. O'Neil, K. T., and DeGrado, W. F. (1990) *Trends. Biochem. Sci. 15*, 59−64.
29. Cheney, R. E., and Mooseker, M. S. (1992) *Curr. Opin. Cell Biol. 4*, 27−35.

30. Rhoads, A. R., and Friedberg, F. (1997) *FASEB J. 11*, 331−340.
31. Olwin, B. B., and Storm, D. R. (1983) *Methods Enzymol. 102*, 148−157.
32. Torok, K., Cowley, D. J., Brandmeier, B. D., Howell, S., Aitken, A., and Trentham, D. R. (1998) *Biochemistry 37*, 6188−6198.
33. Wriggers, W., Mehler, E., Pitici, F., Weinstein, H., and Schulten, K. (1998) *Biophys. J. 74*, 1622−1639.
34. Kuboniwa, H., Tjandra, N., Grzesiek, S., Ren, H., Klee, C. B., and Bax, A. (1995) *Nat. Struct. Biol. 2*, 768−776.
35. Klevit, R. E. (1983) *Methods Enzymol. 102*, 82−104.
36. Comte, M., Maulet, Y., and Cox, J. A. (1983) *Biochem. J. 209*, 269−272.
37. Scaloni, A., Miraglia, N., Orru, S., Amodeo, P., Motta, A., Marino, G., and Pucci, P. (1998) *J. Mol. Biol. 277*, 945−958.
38. Chattopadhyaya, R., Meador, W. E., Means, A. R., and Quiocho, F. A. (1992) *J. Mol. Biol. 228*, 1177−1192.
39. Zhang, M., Tanaka, T., and Ikura, M. (1995) *Nat. Struct. Biol. 2*, 758−767.
40. Hanley, R. M., Means, A. R., Ono, T., Kemp, B. E., Burgin, K. E., Waxham, N., and Kelly, P. T. (1987) *Science 237*, 293−297.
41. Blumenthal, D. K., Charbonneau, H., Edelman, A. M., Hinds, T. R., Rosenberg, G. B., Storm, D. R., Vincenzi, F. F., Beavo, J. A., and Krebs, E. G. (1988) *Biochem. Biophys. Res. Commun. 156*, 860−865.
42. Cimler, B. M., Andreasen, T. J., Andreasen, K. I., and Storm, D. R. (1985) *J. Biol. Chem. 260*, 10784−10788.
43. Alexander, K. A., Wakim, B. T., Doyle, G. S., Walsh, K. A., and Storm, D. R. (1988) *J. Biol. Chem. 263*, 7544−7549.
44. Gerendasy, D. D., Herron, S. R., Jennings, P. A., and Sutcliffe, J. G. (1996) *J. Biol. Chem. 270*, 6741−6750.
45. Brockerhoff, S. E., Stevens, R. C., and Davis, T. N. (1994) *J. Cell Biol. 124*, 315−323.
46. Ikura, M., Clore, G. M., Gronenborn, A. M., Zhu, G., Klee, C. B., and Bax, A. (1992) *Science 256*, 632−638.
47. Chapman, E. R., Alexander, K., Vorherr, T., Carafoli, E., and Storm, D. R. (1992) *Biochemistry 31*, 12819−12825.
48. Urbauer, J. L., Short, J. H., Dow, L. K., and Wand, A. J. (1995) *Biochemistry 34*, 8099−8109.
49. Persechini, A., and Cronk, B. (1999) *J. Biol. Chem. 274*, 6827−6830.
50. Kayano, T., Noda, M., Flockerzi, V., Takahashi, H., and Numa, S. (1988) *FEBS Lett. 228*, 187−194.
51. Dietrich, P. S., McGivern, J. G., Delgado, S. G., Koch, B. D., Eglen, R. M., Hunter, J. C., and Sangameswaran, L. (1998) *J. Neurochem. 70*, 2262−2272.

BI9912600